

Coenzyme Q₀ immobilized on Magnetic Nanoparticle: Synthesis and Antitumoral Effect on Saos, MCF7 and Hela Cell Lines

Mohsen Aboukazempour Amiri^{a, b}, Mahmoud Reza Aghamaali^{a*}, Hadi Parsian^c and Hamed Tashakkorian^{c, d}

^aDepartment of Biology, Faculty of Sciences, University of Guilan, Rasht, Iran. ^bDepartment of Basic Sciences, Mazandaran University of Science & Technology (MUST), Babol, Iran. ^cCellular and Molecular Biology Research Center (CMBRC), Health Research Institute, Babol University of Medical Sciences, Babol, Iran. ^dDepartment of Pharmacology, School of Medicine, Babol University of Medical Sciences, Babol, Iran.

Abstract

Many attempts in medical community focused on the preparation of anticancer agents. Various Coenzyme Q such as CoQ₀ analogs have been reported as anti-inflammatory, anticancer, and antioxidant substances. In this study a novel derivatives of Coenzyme Q as an anticancer agent have been introduced. The prepared magnetic nanoparticle, containing CoQ₀ were prepared using common chemical methods and also characterized by means of nuclear magnetic resonance (NMR), fourier transform infrared (FT-IR), thermal gravimetric analysis (TGA), and differential scanning calorimetric (DSC). To evaluate the antiproliferative effects of the nanoparticle, the prepared compound was treated with cell lines such as Hela, MCF-7 and Saos. Moreover, the outcomes were compared with normal fibroblast cell line. These assessments were performed by means of MTT assay. Investigation on the capability of this prepared nanoparticle showed some reliable results including cytotoxicities against MCF7, Saos and Hela cancer cell lines which were illustrated by displaying the morphology of the treated cells using AO/EB dual staining fluorescent technique. Employing simple method for preparation as well as the promising cytotoxic results makes it as a promising candidate for further bioexperiments.

Keywords: Magnetic Nanoparticles; Coenzyme Q₀; Cancer cells; AO/EB dual staining, Mtt assay.

Introduction

In recent years cancer is one of the most common causes of death. The World Health Organization (WHO) statistics indicate that cancer mortality is increasing worldwide, with an estimation of 13 million deaths in 2030. Early and specific detection as well as systematic screening play a significant role in cancer prevention and treatment (1, 2). Primary

treatments are included chemotherapeutic compounds and ionizing radiation for elimination of the cancer tumor mass. These treatments do not greatly differentiate between cancerous and normal cells, leading to systemic toxicity and adverse effects, limiting the maximum dose of drug (3). So, emerging novel therapeutic agents are highly required. Potential anticancer drugs need to be identified from alternative sources, such as natural products (4) and Peptide-based drugs (5, 6). Due to advantages of the peptide

* Corresponding author:
E-mail: aghamaali@guilan.ac.ir

molecules, including small molecular size, high activity, low immunogenicity, diversity of sequence, appreciable biocompatibility and modification sites for possible functionalization, Peptide-based drugs gained much interest (7). Over the last two decades, a large number of nanoparticulate drug delivery systems consisting of organic or inorganic materials have been evaluated for cancer therapy (8). The use of nanoparticles in drug delivery is a process of drug transition with an ultimate goal to deliver most of administered drug to the target sites, such as tumor tissues, while eliminating the drug accumulation at non-target sites. Thus, tremendous efforts have been made to develop targeted drug delivery systems during the past decade (9, 10). Nanocarrier (NC) drug delivery, such as liposome, polymeric nanoparticle and micelles, nanoshells, dendrimer, inorganic/metallic nanoparticles, and magnetic and bacterial nanoparticles, represents an exciting and promising strategy to effectively treat a wide range of diseases including cancer (11-13).

Nanoparticles have many advantages as drug carrier agents; however, there are still several limitations, such as instability in circulation, distribution inadequate tissue, poor oral bioavailability, and toxicity (11). For tumor cell targeting, NCs have to conquer a series of obstacles, which can be classified as systemic targeting and intracellular targeting stages, to guide therapeutic agent to its therapeutic target (12). The systemic barriers include stability and survival in the bloodstream, prolonged circulation time, preferential surrounding and accumulation at tumor tissue, while the intracellular barriers involve the specific binding to the tumor cells and internalization of the drug-carriers by endocytosis, endo/lysosomal escape, cytosolic localization, and controllable drug release (14, 15). Based on their chemical composition, nanoparticles are broadly divided into two main groups: organic materials such as liposomes, carbon nanotubes, emulsions, dendrimers; and inorganic materials such as metals (16).

Among the successes, magnetic

nanoparticles (*e.g.*, magnetite Fe_3O_4 or maghemite Fe_2O_3) appear to be quite suitable for being a drug targeted carrier, due to their capability of delivering pharmaceuticals to a specific site of the body by means of a gradient magnetic field (17-19). Iron oxide (or magnetite) nanoparticles with nanocrystalline magnetite (Fe_3O_4) cores due to their biocompatibility, facile synthesis, and biodegradability may be used for specific application and oncological medicine (20). The ability to quickly turn off drug delivery, by simple removing the external magnetic field is the most important advantage of magnetic drug targeting over conventional controlled release formulations (21). Also, magnetic nanoparticles can improve local action of the drug and minimize the side effects to the patient (22). Furthermore, a lot of unique properties, such as small size (~100 nm) allow them to function at the cellular level, super paramagnetism, high magnetization, and large specific surface area (23).

Coenzyme Q (CoQ) is a well-known biomolecule, comprises of a quinone nucleus and a hydrophobic side chain containing variable number of trans isoprenoid units (24). Coenzyme Q_0 (Co Q_0 , 2, 3-dimethoxy-5-methyl-1,4-benzoquinone), a novel quinone derivative without isoprenoid side chain, inhibits the activity of complex 1 of mitochondrial respiratory chain and prevent opening of the mitochondrial permeability transition pore (PTP) (25). Some studies reported that Co Q_0 have a potent anti-oxidant effects and anti-cancer activity against human breast cancer cells through induction of apoptosis and cell-cycle arrest. The other researches presented potent cytotoxicity of Co Q_0 towards insulin producing cells and also human breast cancer cells (26, 27). In spite of its cytotoxicity, some *in-vivo* studies have proved no injurious effects of Co Q_0 when joined with other nutrients. Significantly, administration of Co Q_0 mixture prevents oxidative damage in heart, blood, kidney, liver, and spleen of rodents (28, 29). The aim of this study was appraisal of the cytotoxic effects of synthesized nanoparticles containing Coenzyme Q_0 on several cancer cell lines

which include Fibroblast, Saos, MCF-7, and Hela cell lines.

Experimental

Chemicals involving solvents, Coenzyme Q_0 (2,3-Dimethoxy-5-methyl-p-benzoquinone), ammonia solution (25%), (3-Mercaptopropyl) and trimethoxysilane were acquired from sigma (Switzerland) Company. Iron (II) chloride and Iron (III) chloride and tetraethyl ortho silicate were purchased from Merck (Germany) Company. All the chemicals were used without further purification.

Equipment

^1H NMR spectrum was recorded on a Bruker 400 MHz. IR spectra were recorded on a Perkin-Elmer FT-IR-1710 spectrophotometer with the samples in KBr pellets. The plates of biological samples were read using Elisa reader (Ratio-China) at 570 nm. Biological results were calculated statistically using SPSS 17 and Microsoft Excel and presented as mean \pm SD in triplicate experiment. Differences in the results were determined at significant difference of 0.05 ($P \leq 0.05$). FESEM was recorded on a Hitachi S4160 instrument (Tokyo, Japan). TGA were determined using Perkin-Elmer Pyris Diamond and Pyris 6 TGA Consumables, respectively under a nitrogen atmosphere at a heating rate of $10\text{ }^\circ\text{C min}^{-1}$.

Synthesis of conjugated 3-(trimethoxysilyl) propane-1-thiol to 2,3,5-trimethoxycyclohexa-2,5-diene-1,4-dione (Q_0) (Silanized Q_0):

For the synthesis of the silanized Q_0 , firstly, 0.024 g Na was dissolved in 10 cc methanol and then 3-(trimethoxysilyl)propane-1-thiol (0.2 cc, 1.06 mmol) was added to the methoxide/methanol solution, and after 30 min Q_0 (0.194 gr, 1.06 mmol) was added to the prepared mixture. Color of the solution was changed from light to dark brown. The reaction stayed at the same condition overnight under N_2 atmosphere. Then, methanol was evaporated under reduced pressure and crude brown solid was washed at first with methanol to remove sodium methoxide and then with acetone for removal of excess raw materials to reach the pure silanized Q_0 (0.3 gr).

IR (as KBr pellet): 683 cm^{-1} (C-S bond), 1112 cm^{-1} (broad peak related to C-O and Si-O bonds), 1250 cm^{-1} (C-C bond), 1331 cm^{-1} (CH_3 groups), 1460 cm^{-1} (CH_2 group), 1645 cm^{-1} (C = C bond), 1693 and 1750 cm^{-1} (C = O bond), 2930 cm^{-1} (C-H).

^1H NMR: 0.91 ppm (t, CH_2), 1.05 ppm (q, CH_2), 1.24 ppm (t, CH_2), 1.65 ppm (s, Si-OMe), 3.17 ppm (s, -OMe), 3.56 ppm (s, -OMe), 3.75 ppm (d, C-H), 3.95 ppm (d, C-H).

Preparation of $\text{Fe}_3\text{O}_4\text{-SiO}_2$ (Silicated Fe_3O_4)

For preparation of the silicated nanomagnetic particles, 2 gr Fe_3O_4 (22) was dispersed on 50 cc distilled water and sonicated for 15 min. Then, 1 cc TEOS solved in 9 cc distilled water, added to the aqueous mixture of the Fe_3O_4 , 3 gr glycerol and also some drops of glacial acetic acid were added to the mixture to reach the pH 4.5. To reach the temperature up to $90\text{ }^\circ\text{C}$, agitation of the mixture was continued for 2 h. Then, silicated nanomagnetic particles were removed by magnet and washed three times with water and acetone respectively to remove any non-supported material and reagents. The nanoparticles were dried in vacuum at $50\text{ }^\circ\text{C}$ overnight (2.8 gr).

IR (as KBr pellet): $550\text{-}600\text{ cm}^{-1}$ (Fe-O-Fe bond), $1050\text{-}1100\text{ cm}^{-1}$ (broad peak related to Si-O bonds), $3400\text{-}3500\text{ cm}^{-1}$ (O-H bonds)

Preparation of the immobilized Q_0 onto the silicated Fe_3O_4 ($\text{Fe}_3\text{O}_4\text{-SiO}_2\text{-}Q_0$)

0.6 g of the silicated Fe_3O_4 was added to the 25 cc H_2O and sonicated for 15 min. Then 0.3 gr (0.79 mmol) silanized Q_0 that had been solved in 2 cc DMSO was added to the mixture. 1.5 cc glycerol and some drops of acetic acid were added to the above mixture to reach to the pH 4.5. After that, the mixture stirred for 2 h at $90\text{ }^\circ\text{C}$. Then, by using magnet, the synthesized particles were collected and washed with DMSO, water, and acetone. At the end, wet powder was dried in vacuum oven at $40\text{ }^\circ\text{C}$ overnight (0.8 gr).

IR (as KBr pellet): about 630 cm^{-1} (Fe-O-Fe bond), 1038 cm^{-1} (broad peak related to C-O and Si-O bonds), 1425 cm^{-1} (CH_2 group), 1632 cm^{-1} (C = C bond), 1745 cm^{-1} (C = O bond), 2925 cm^{-1} (C-H bond), 3421 cm^{-1} (O-H bond).

Cell culture

The cell culture and primary human Fibroblasts isolation were performed according to the previous published article (28). Briefly, The HeLa (The human cervix cancer cell line), Saos (Sarcoma osteogenic cells), and MCF-7 (human breast adenocarcinoma cell line) were obtained from national cell bank of Iran (NCBI, Pasteur Institute of Iran). In 5% CO₂ at 37 °C with 95% humidity of air, the cell lines were cultured in RPMI-1640 (Sigma-Aldrich, Germany) and fortified with 10% fetal bovine serum FBS (Gibco/Invitrogen), and 1% penicillin and streptomycin (Sigma-Aldrich, USA). After washing with PBS, the culture medium was changed each two days. This process was completed with 10 mL of fresh culture medium for 2-5 passage.

MTT Assay

The HeLa, MCF-7, and Saos cell lines were cultured in 96-well plates (10⁴ cells/well). Afterwards, 200 µL culture medium containing 10% (µg/mL) FBS was added to each wells. Under standard protocol, the culture medium was removed and the cells were treated with fresh ones containing different concentration of nanoparticles. After being in an incubator for 24, 48, and 72 h, 200 µL of the culture medium was removed and 50 µL of MTT (5mg/mL) solution was added to the wells. After appropriate time, the previous MTT solution was replaced with 200 µL of MTT solvent (acidic isopropanol) for solubilization of the formazan crystals. Subsequently, the mean absorbance of the plate was measured using elisa reader at 570 nm.

Results

Chemical preparation of the nanocomposite based material, specifically magnetic nanoparticles, is a known method for the introducing the novel material with fantastic properties. Moreover, immobilization of the biological materials onto the inorganic safe nanoparticles is a modern technique to save dosage in the ordinary usage for any targets. In this regard, the present project was studied for the preparation of the biologically significant compound, Q₀, immobilized on the silanized Fe₃O₄ and studying of its corresponding anticancer activity. At the first, Q₀ silanized

was prepared by Michael addition of the 3-(trimethoxysilyl) propane-1-thiol to Q₀ in the presence of sodium methoxide whose result was confirmed by FT-IR and NMR (Scheme 1). Its FT-IR spectrum (Figure 1) showed indexed peaks at 683 cm⁻¹ (C-S bond), 1112 cm⁻¹ (broad peak related to C-O and Si-O bond), 1250 cm⁻¹ (C-C bond), 1331 cm⁻¹ (CH₃ groups), 1460 cm⁻¹ (CH₂ group), 1645 cm⁻¹ (C = C bond), 1693 (C = O bond), 2930 cm⁻¹ (C-H) and also, its NMR spectrum (Figure 2) with some peaks at 0.91 ppm (t, CH₂), 1.05 ppm (q, CH₂), 1.24 ppm (t, CH₂), 1.65 ppm (s, Si-OMe), 3.17 ppm (s, -OMe), 3.56 ppm (s, -OMe), 3.75 ppm (d, C-H), and 3.95 ppm (d, C-H) confirmed successful preparation of the Q₀ silanized.

To have more functionalized nanoparticles, we coated the Fe₃O₄ nanoparticles with tetraethyl ortho silicate and then silanized CoQ₀ was added. The FTIR spectrum of the coated magnetic nanoparticles was shown in (Figure 3). For performing the last step, Q₀ silanized was added to the prepared Fe₃O₄-SiO₂ for chemical bonding and synthesis of the Fe₃O₄-SiO₂-Q₀ (Scheme 2). FT-IR of the synthesized compound (Figure 4) displayed characteristic peaks at about 630 cm⁻¹ (Fe-O-Fe bond), 1038 cm⁻¹ (broad peak related to C-O and Si-O bonds), 1425 cm⁻¹ (CH₂ group), 1632 cm⁻¹ (C = C bond), 1745 cm⁻¹ (C = O bond), 2925 cm⁻¹ (C-H bond), and 3421 cm⁻¹ (O-H bond), that their correlations were reasonable and structure confirming.

SEM and EDS

The morphologies and size of synthesized materials Fe₃O₄-SiO₂-Q₀ was investigated by SEM. (Figure 5) demonstrated SEM images of Fe₃O₄-SiO₂-Q₀ nanocomposite in 200 and 100 nm magnification. It can be observed that the synthesized nanocomposite has a sphere like shape with diameter ranging below 50 nm which is significant for bioapplications. Also, EDS experiment which was shown in (Figure 6), clearly confirmed the presence of the mentioned elements in the final composite.

Thermal properties

TGA and DTG

Thermogravimetric Analysis (TGA) of the

prepared nanoparticle was evaluated. After salinization of the magnetic nanoparticles and further immobilization of CoQ_0 , thermal analysis was performed under N_2 atmosphere, from room temperature to $600\text{ }^\circ\text{C}$. As presented in (Figure 7), also, the Derivative Thermogravimetric Analysis (DTG) curve for both thermogram exhibited that the prepared nanoparticle has one main stage weight loss more than solvent removal stage below $100\text{ }^\circ\text{C}$ at around $280\text{ }^\circ\text{C}$. This weight loss is due to the presence of organic structures in the nanoparticles which were around 27.5%. Moreover, according to the TGA curves, the amount of inorganic excess materials containing Fe_3O_4 and silane groups was around 72.5%.

The effects of nanoparticles containing CoQ_0 on the proliferation of cancer cell lines (Fibroblast, Saos, MCF-7 and Hela) were investigated by MTT assay.

Inhibition of cell proliferation by CoQ_0 on fibroblast cells

As can be seen in (Figures 8), cell proliferation of the treated fibroblast cells with nanoparticles containing CoQ_0 was decreased. This effect resulted in the morphological changes (Figure 9) after 24, and 72 h in a dose-dependent manner. Fibroblast cells that exposed to nanoparticles containing CoQ_0 exhibited an IC_{50} about $250\text{ }\mu\text{M}$ for all three mentioned times as compared to the control cells (Nanoparticles without CoQ_0).

Inhibition of cell proliferation by CoQ_0 on saos cells

(Figure 10) displays the treated saos cells with nanoparticles, containing CoQ_0 which resulted in the significant decrease in

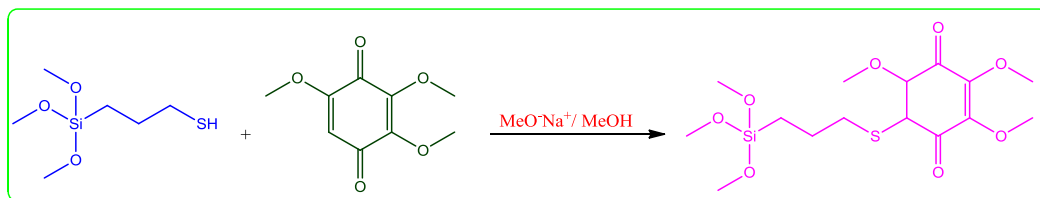
cell proliferation. This reduction resulted in morphological changes after 24, 48, and 72 h in a dose-dependent manner. Saos cells, exposed to nanoparticles containing CoQ_0 exhibiting an IC_{50} about $250\text{ }\mu\text{M}$ for 24 and 72 h and an IC_{50} about $125\text{ }\mu\text{M}$ for 48 h as compared to the control cells. Evaluation of apoptosis incidence and morphological observation of Saos cells treated with nanoparticles was conducted using AO/EB staining technique (Figure 11).

Inhibition of cell proliferation by CoQ_0 on MCF-7 cells

(Figures 12) demonstrated that the treated MCF-7 cells with nanoparticles containing CoQ_0 caused the reduction in cell proliferation. This dose dependent effect resulted in morphological changes and evaluated using AO/EB staining technique (Figure 13). MCF-7 cells, exposed to nanoparticles containing CoQ_0 exhibited IC_{50} about $62.5\text{ }\mu\text{M}$ for 24 and 48 h and an IC_{50} about $250\text{ }\mu\text{M}$ for 48 h as compared to the control cells.

Inhibition of cell proliferation by CoQ_0 on Hela cells

(Figures 14) show the treated Hela cells with nanoparticles containing CoQ_0 . The decrease in cell proliferation consequently resulted in morphological changes after 24, 48, and 72 h in a dose-dependent manner. Hela cells, exposed to nanoparticles containing CoQ_0 exhibited an IC_{50} about $500\text{ }\mu\text{M}$ in all of the three mentioned times as compared to the control cells. Evaluation of apoptosis incidence and morphological observation of Hela cells treated with nanoparticles containing CoQ_0 conducted using AO/EB staining technique (Figure 15).



Scheme 1. Synthesis of silanized Q_0 .

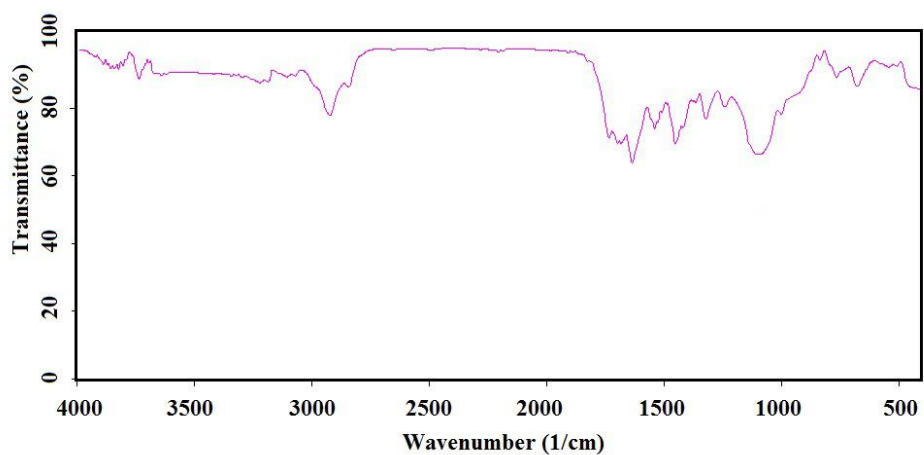


Figure 1. FTIR spectrum of the Silanized Q₀.

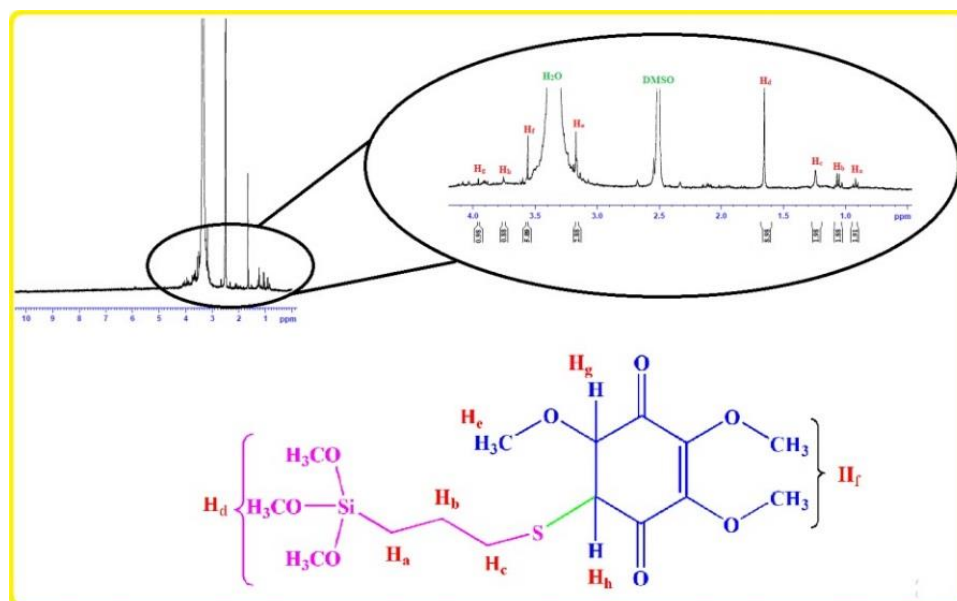


Figure 2. ¹H NMR of the synthesized Silanized Q₀.



Scheme 2. Synthesis of $Fe_3O_4-SiO_2-Q_0$.

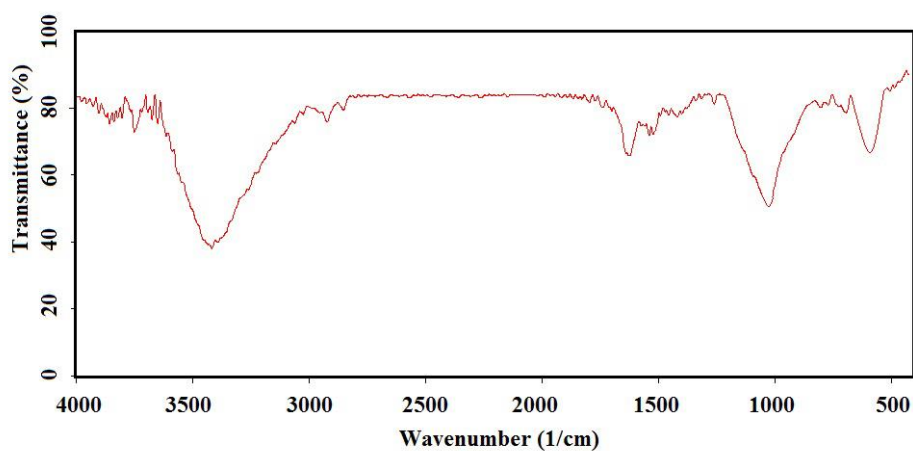


Figure 3. FTIR spectrum of the silicated Fe_3O_4 .

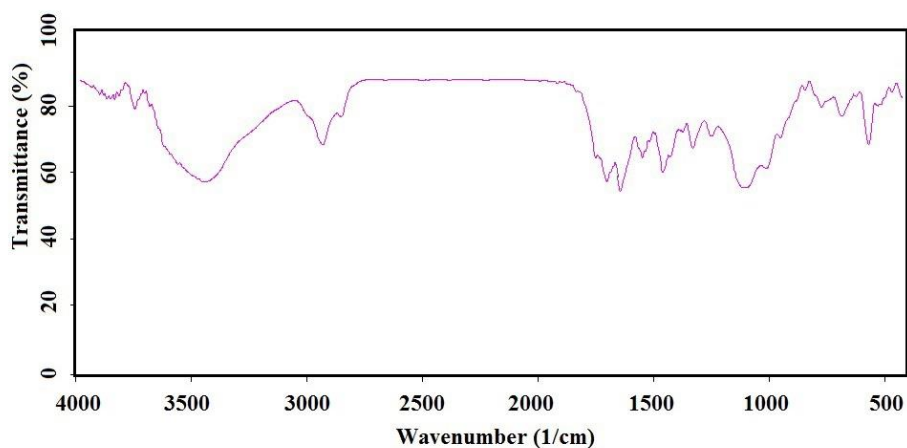


Figure 4. FTIR spectrum of the prepared magnetic nanoparticle functionalized with CoQ_0 .

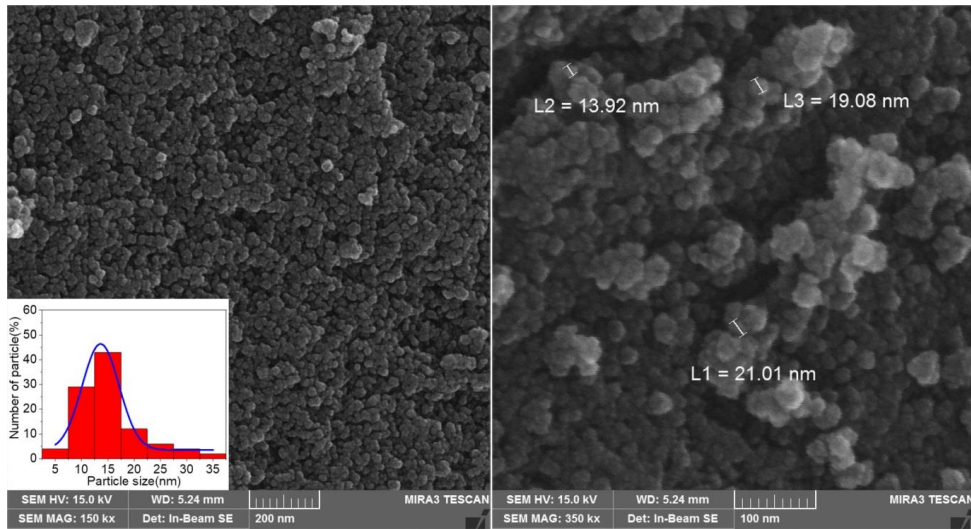


Figure 5. SEM of the magnetic nanoparticle in the scale of 200 and 100 nm.

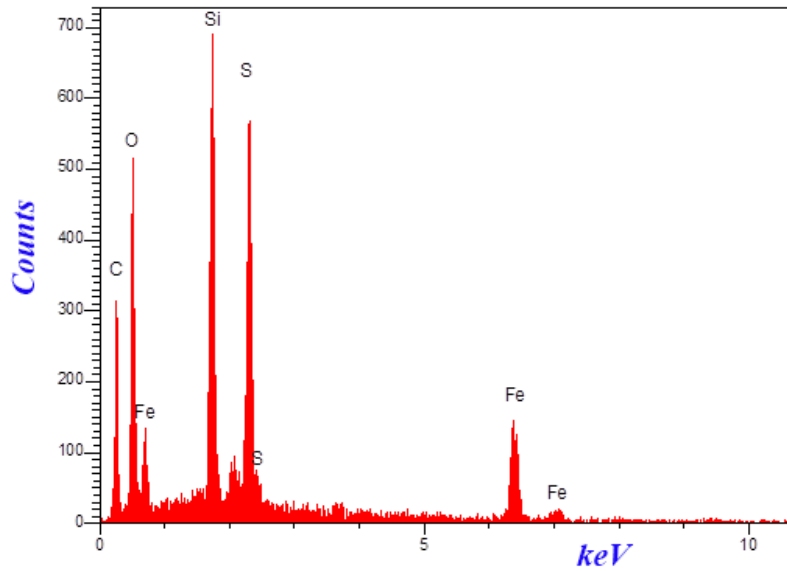


Figure 6. EDS of the nanoparticles containing CoQ₀.

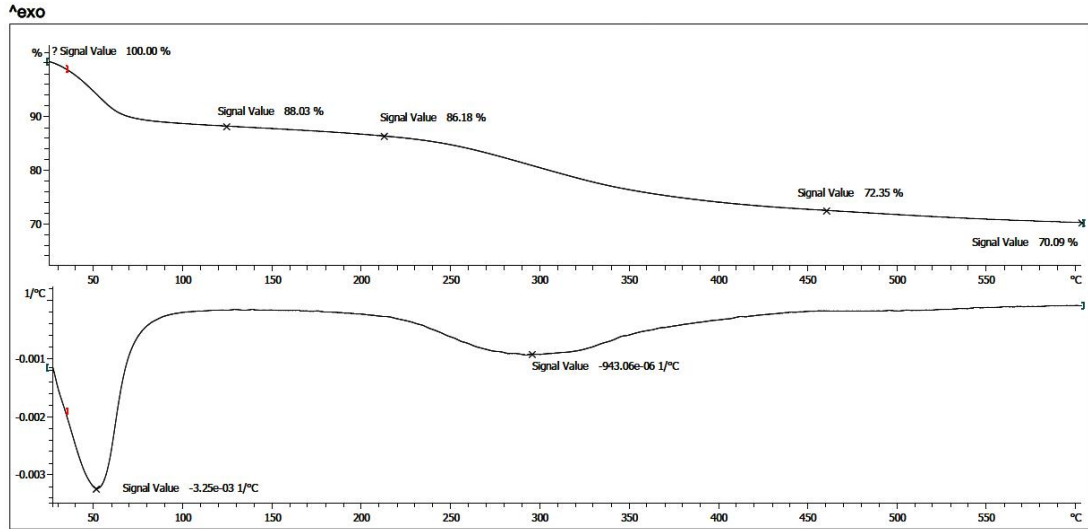


Figure 7. TGA and DTG curves of the synthesized magnetic nanoparticle.

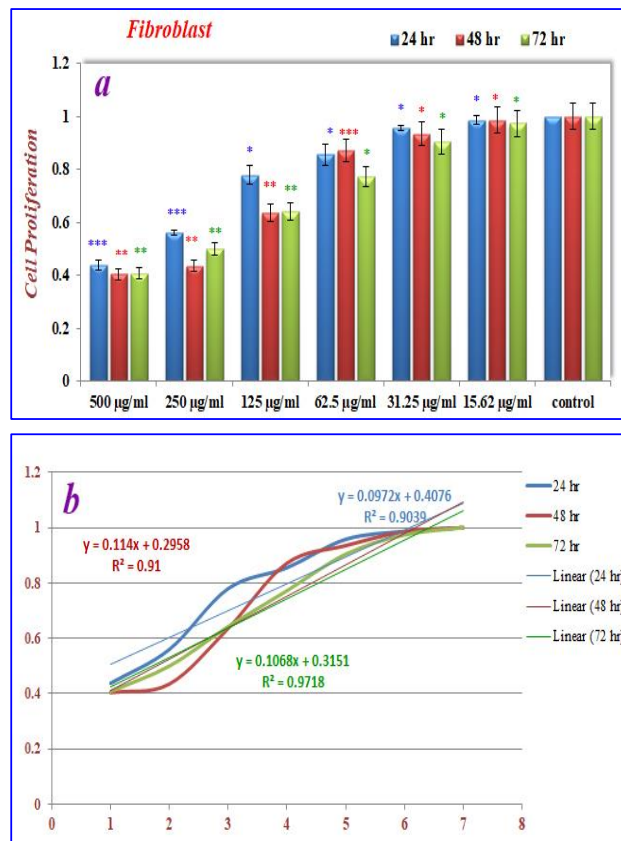


Figure 8. (a) The inhibition of cell proliferation by different concentrations of nanoparticles containing CoQ_0 as compared to the control cells in 24, 48 and 72 h. Each bar represents the mean \pm standard deviation of three independent tests. * $P < .05$; ** $P < .01$; *** $P < .001$ compared with untreated control cells.

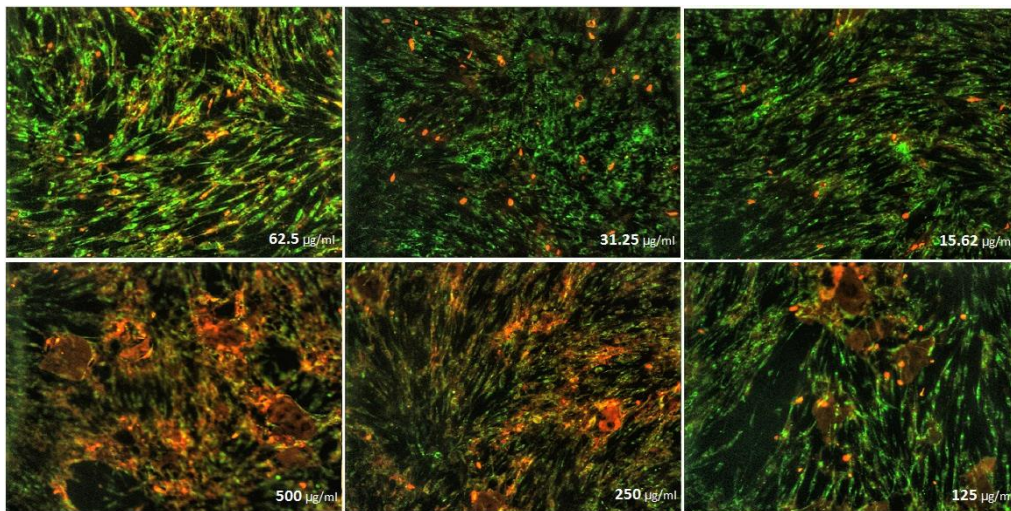


Figure 9. Cell Morphology: Evaluation of apoptosis incidence and morphological observation of Fibroblast treated with nanoparticles containing CoQ₀ using AO/EB staining at × 400 magnifications. Early apoptotic cells (chromatin condensation stained green); late apoptotic cells (chromatin condensation stained orange); membrane blebbing; shrunken and loss of membrane shapes are can be seen in the (Figures). The higher the concentration of CoQ₀ nanoparticles used the more aggressive induction of death in the cancer cells.

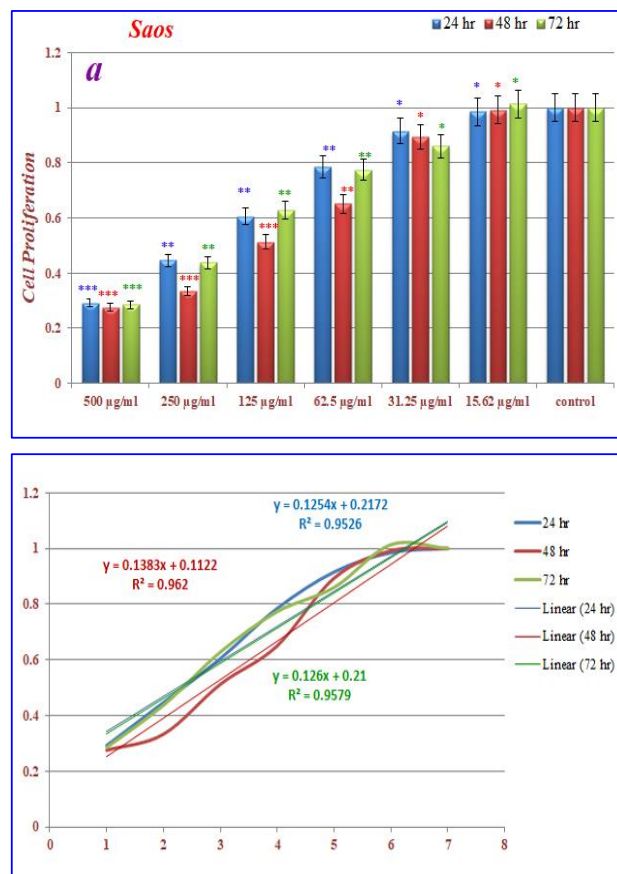


Figure 10. The inhibition of cell proliferation by different concentrations of nanoparticles containing CoQ₀ as compared to the control cells in 24, 48 and 72 h. Each bar represents the mean ± standard deviation of three independent. **P* < 05; ***P* < 01; ****P* < 001 compared with untreated control cells.

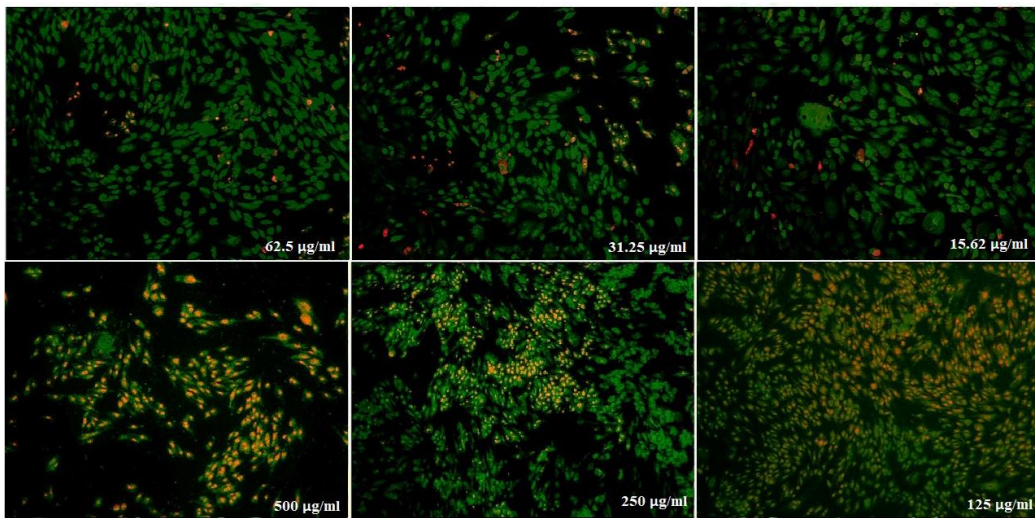


Figure 11. Cell Morphology: Evaluation of apoptosis incidence and morphological observation of Saos treated with nanoparticles containing CoQ_{10} using AO/EB staining at $\times 400$ magnifications. Early apoptotic cells (chromatin condensation stained green); late apoptotic cells (chromatin condensation stained orange); membrane blebbing; shrunken and loss of membrane shapes are can be seen in the Figures. The higher the concentration of CoQ_{10} nanoparticles used the more aggressive induction of death in the cancer cells.

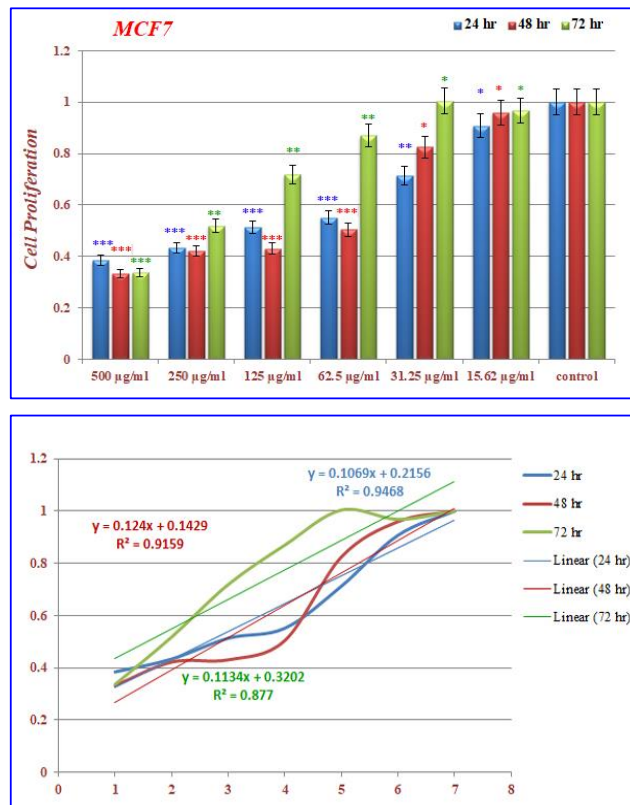


Figure 12. The inhibition of cell proliferation by different concentrations of nanoparticles containing CoQ_{10} as compared to the control cells in 24, 48 and 72 h. Each bar represents the mean \pm standard deviation of three independent. $*P < 0.05$; $**P < 0.01$; $***P < 0.001$ compared with untreated control cells.

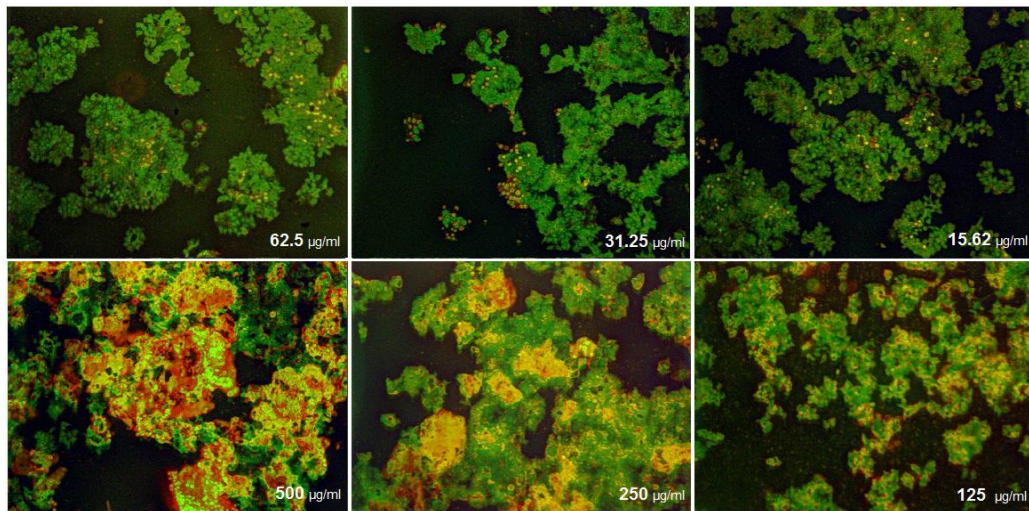


Figure 13. Cell Morphology: Evaluation of apoptosis incidence and morphological observation of MCF7 treated with nanoparticles containing CoQ₀ using AO/EB staining at × 400 magnifications. Early apoptotic cells (chromatin condensation stained green); late apoptotic cells (chromatin condensation stained orange); membrane blebbing; shrunken and loss of membrane shapes are can be seen in the Figures. The higher the concentration of CoQ₀ nanoparticles used the more aggressive induction of death in the cancer cells.

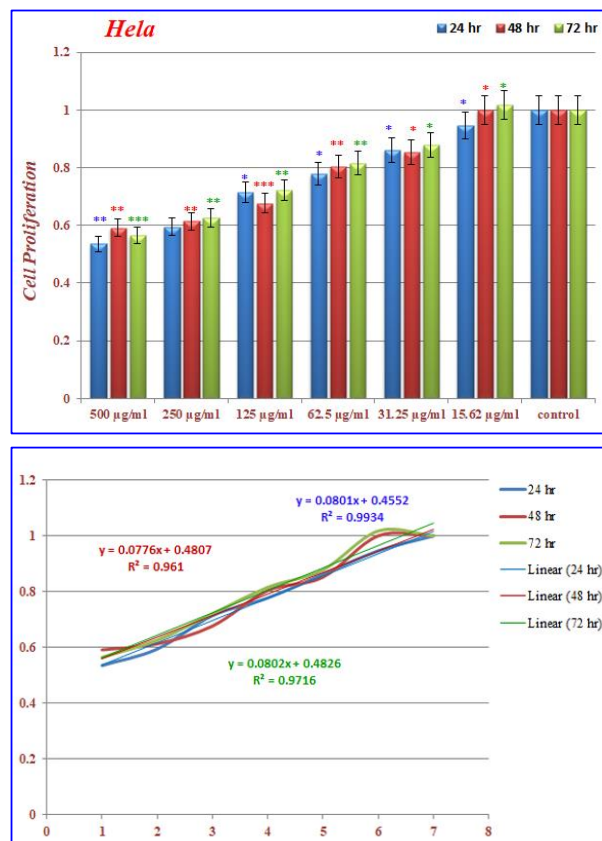


Figure 14. The inhibition of cell proliferation by different concentrations of nanoparticles containing CoQ0 as compared to the control cells in 24, 48 and 72 h. Each bar represents the mean ± standard deviation of three independent. **P* < 05; ***P* < 01; ****P* < 001 compared with untreated control cells.

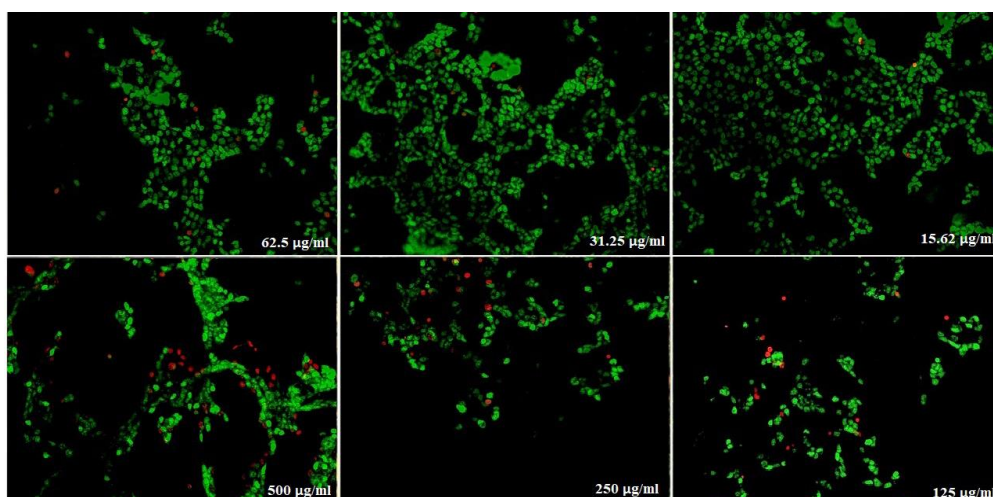


Figure 15. Cell Morphology: Evaluation of apoptosis incidence and morphological observation of HeLa treated with nanoparticles containing CoQ_0 using AO/EB staining at $\times 400$ magnifications. Early apoptotic cells (chromatin condensation stained green); late apoptotic cells (chromatin condensation stained orange); membrane blebbing; shrunken and loss of membrane shapes are can be seen in the Figures. The higher the concentration of CoQ_0 nanoparticles used the more aggressive induction of death in the cancer cells.

Discussion

Due to the fact that cancer is one of the most common causes of death in the world, many efforts in the medical community have focused on the development of anticancer drugs (30). Currently, the cancer is treated with surgery, radiotherapy, chemotherapy, targeted therapy, hormonal therapy, and immunotherapy modalities, but all of them carry some side effects and shortcomings such as drug resistance, severe adverse reactions, moderate therapeutic efficacy, low concentration of therapeutics at the site of action and/or fast renal clearance of conventional drugs, etc. The reason for these shortcomings and side-effects are mostly due to non-specificity and systemic toxicity of anti-cancer drugs(31, 32).

Over the past few years, the use of nanoparticles has gained tremendous interest, because nanoparticles, by using both passive and active targeting strategies, can enhance the intracellular concentration of drugs in cancer cells while avoiding toxicity in normal cells (11, 33). Various coenzyme Q (CoQ) analogs have been reported as anti-inflammatory, anticancer, and antioxidant substances. Coenzyme Q_0 (CoQ_0 or Ubiquinone 0) is a redox-active ubiquinone compound that

accumulates predominantly in mitochondria and also is a potent inhibitor than all other quinone analogs (34). In previous *in-vitro* and *in-vivo* studies have shown that CoQ_0 has many biological effects on cancer cells, such as cell cycle arrest, apoptosis, and anti-tumorigenic activity (26).

In this study, we investigate the anticancer effect of nanoparticles containing CoQ_0 on some different common cancer cell lines. The results of the present study indicated that the nanoparticles containing CoQ_0 could be an anti-cancer agent according to the proposed schematic mechanism of the anticancer activity of Coenzyme Q0 immobilized on magnetic nanoparticle (Figure 16).

Furthermore, the immobilized CoQ_0 has shown a strong potential anti-proliferative effects on several cancer cell lines as reported by the other investigators (26). Dose and time dependency as well as the effect of the types of the cell lines on cells proliferation through the MTT assay were investigated in this article.

CoQ_0 treatment also resulted in the decrease in cell viabilities in A549 (lung cancer cells), HepG2 (HepG2 hepatoma cells), and SW480 (colon cancer cells) cancer cell lines. Moreover, study on A549 lung cancer cells indicated that CoQ_0 induced reactive oxygen

species (ROS) generation and apoptosis in A549 cells, inhibited by the antioxidant ascorbic acid (35).

Our findings demonstrated a reduction in cells viabilities, when compared with the control cells after treatment with different doses of nanoparticles in several cancer cell lines for 24, 48, and 72 h. The increase in concentrations of the nanoparticles containing CoQ₀ samples will result in the significant decrease in proliferation of the all mentioned cancer cell lines.

In addition, it is reported that cell viabilities dramatically decreased when the MCF-7 cells were treated with CoQ₀. CoQ₀ in the presence of ultraviolet B induced apoptosis in human breast cancer cells. The treatment using CoQ₀ moderately inhibits the growth of breast cancer MCF-7 cells, and the cell viability was significantly decreased when the cells were pretreated with UVB irradiation (29).

Several studies have examined various mechanisms for CoQ₀ performance. A study showed that non-cytotoxic concentration of CoQ₀ exhibits anti-inflammatory and antioxidant properties against LPS (lipopolysaccharide) challenge and

pharmacological actions of CoQ₀ are mediated via inhibition of NFκB/AP-1 activation and induction of Nrf2/ARE signaling. MTT result of another study showed that CoQ₀ treatment for 24 h did not affect the viability of macrophages up to 10 μM concentration, whereas a significant reduction (p b 0.05) was observed with 15 and 20 μM concentrations (27).

Published studies showed that efficacy of CoQ₀ in cell growth inhibition, induction of apoptosis, and prevention of metastasis may be due to suppression of the Wnt/β-catenin signaling pathway in melanoma cells. Additionally, according to the previous articles, effects of CoQ₀ on the proliferation of murine melanoma cell lines (B16F10, B16F1, and A2058) were determined by MTT assay. CoQ₀ exhibits a significant cytotoxic effect on melanoma cell lines (B16F10, B16F1, and A2058), while causing little toxicity toward normal (HaCaT) cells. These results demonstrate that CoQ₀ were more potent towards the cancer cells than the normal ones.⁽³¹⁾ In addition, previous studies have indicated an important issue that CoQ₀ through suppression of MMP-9/ICAM-1/

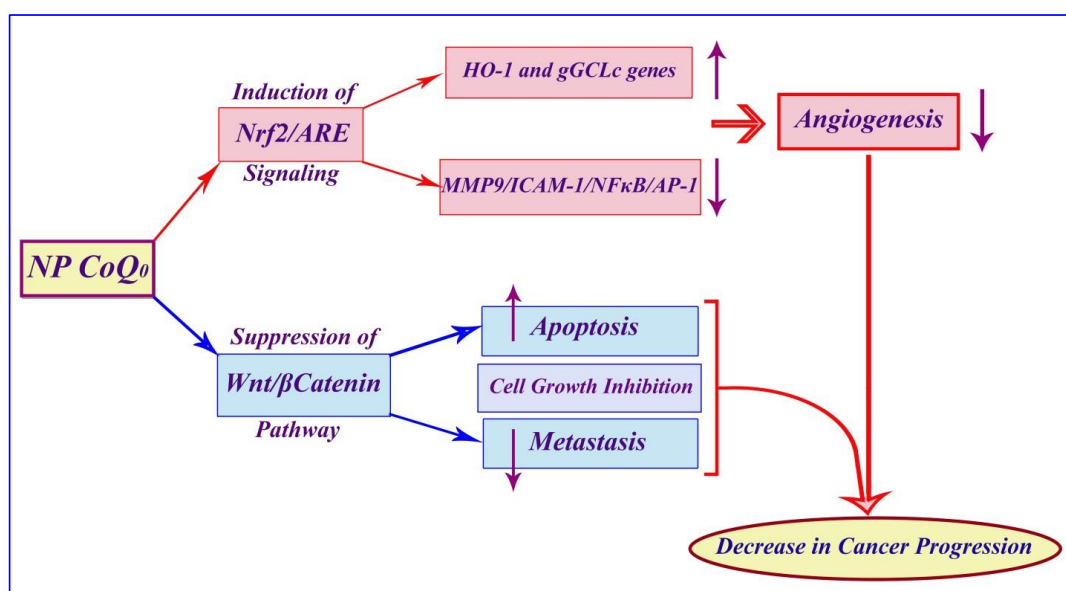


Figure 16. The proposed mechanism of anticancer activity of Coenzyme Q0 immobilized on magnetic nanoparticle against cancer cells.

NF- κ B, activation and up regulation of HO-1 and g-GCLC genes, both via Nrf2/ARE signaling cascades in TNF- α -activated human endothelial cells, causes anti-angiogenic properties. Cell viability results from the MTT tested concentrations (2.5, 5 and 10 mM) in a study showed that up to 10 mM of CoQ₀ had no adverse effects on endothelial cell number (28).

It is reported that MCF-7 cells were exposed to 0 to 35 μ M of CoQ₀ for 24 to 72 h. Treating MCF-7 cells with 35 μ M CoQ₀ for 24 and 48 h had no significant effects on cell viabilities. However, cell viability dramatically decreased when the MCF-7 cells were treated with CoQ₀ (35 μ M) for 72 h (29).

Conclusion

In recent years, researchers have focused on the preparation of derivatives of biomolecules. Incorporating nanoparticles as a biomolecule's base, can exhibit some promising characteristics. On the basis of this hypothesis, we designed a study to survey on the cytotoxic characteristics of magnetic nanoparticles containing CoQ₀. After preparation of the mentioned nanoparticles and appraisal of the structural characterization, by incorporation of the MTT assay, findings indicate that nanoparticles containing CoQ₀ have cytotoxic effects on several known cancer cell lines when compared with the nanoparticles without CoQ₀. Evaluation of apoptosis incidence and morphological observation were also detected by AO/EB staining method. Moreover; thermophysical properties were investigated thoroughly. These results demonstrated that these magnetic nanoparticles have noteworthy potential which makes it a trustworthy compound for certain bioapplications.

Acknowledgments

The authors gratefully acknowledge the support of the University of Guilan as well as Babol University of Medical Sciences.

References

- (1) Brannon Peppas L and Blanchette JO. Nanoparticle and targeted systems for cancer therapy. *Adv. Drug Deliv. Rev.* (2012) 64: 206-12.
- (2) Feng SS and Chien S. Chemotherapeutic engineering: application and further development of chemical engineering principles for chemotherapy of cancer and other diseases. *Chem. Eng. Sci.* (2003) 58: 4087-114.
- (3) Sinha R, Kim GJ, Nie S and Shin DM. Nanotechnology in cancer therapeutics: bioconjugated nanoparticles for drug delivery. *Mol. Cancer Ther.* (2006) 5: 1909-17.
- (4) Nurhadi Illian D, Zaitun Hasibuan PA, Sumardi S, Nuryawan A, Wati R and Basyuni M. Anticancer activity of polyisoprenoids from avicennia alba blume. in widr cells. *Iran. J. Pharm. Res.* (2019) 18: 1477-87.
- (5) Baharloui M, Mirshokraee SA, Monfared A and Houshdar Tehrani MH. Design and synthesis of novel triazole-based peptide analogues as anticancer agents. *Iran. J. Pharm. Res.* (2019) 18: 1299-308.
- (6) Kheirandish Zarandi P, Zare Mirakabadi A and Sotoodehnejad nematalahi F. Cytotoxic and anticancer effects of icd-85 (venom derived peptides) in human breast adenocarcinoma and normal human dermal fibroblasts. *Iran. J. Pharm. Res.* (2019) 18: 232-40.
- (7) Soleimani M, Mirmohammad Sadeghi H and Jahanian Najafabadi A. A bi-functional targeted P28-NRC Chimeric protein with enhanced cytotoxic effects on breast cancer cell lines. *Iran. J. Pharm. Res.* (2019) 18: 735-44.
- (8) Farokhzad OC and Langer R. Impact of nanotechnology on drug delivery. *ACS Nano.* (2009) 3: 16-20.
- (9) Torchilin VP. Recent approaches to intracellular delivery of drugs and DNA and organelle targeting. *Annu. Rev. Biomed. Eng.* (2006) 8: 343-75.
- (10) Nori A and Kopecek J. Intracellular targeting of polymer-bound drugs for cancer chemotherapy. *Adv. Drug Deliv. Rev.* (2005) 57: 609-36.
- (11) Cho K, Wang X, Nie S, Chen Z and Shin DM. Therapeutic nanoparticles for drug delivery in cancer. *Clin. Cancer Res.* (2008) 14: 1310-6.
- (12) Bae YH and Park K. Targeted drug delivery to tumors: myths, reality and possibility. *J. Control. Release* (2011) 153: 198-205.
- (13) Akbarian M, Mahjoub S, Elahi SM, Zabihi E and Tashakkorian H. Green synthesis, formulation and biological evaluation of a novel ZnO nanocarrier loaded with paclitaxel as drug delivery system on MCF-7 cell line. *Colloids Surf. B Biointerfaces* (2020) 186: 110686.
- (14) Cheng R, Feng F, Meng F, Deng C, Feijen J and Zhong Z. Glutathione-responsive nano-vehicles as a promising platform for targeted intracellular drug and gene delivery. *J. Control. Release* (2011) 152:

- 2-12.
- (15) Panyam J and Labhasetwar V. Biodegradable nanoparticles for drug and gene delivery to cells and tissue. *Adv. Drug Deliv. Rev.* (2003) 55: 329-47.
- (16) Karim E, Rosli R and Chowdhury EH. Systemic delivery of nanoformulations of anti-cancer drugs with therapeutic potency in animal models of cancer. *Curr. Cancer Ther. Rev.* (2016) 12: 204-20.
- (17) Silva AKA, Silva EL, Carvalho JF, Pontes TRF, Neto RPdA, Carriço AdS and Egito EST. Drug targeting and other recent applications of magnetic carriers in therapeutics. *Key Eng. Materials* (2010) 441: 357-78.
- (18) Chomoucka J, Drbohlavova J, Huska D, Adam V, Kizek R and Hubalek J. Magnetic nanoparticles and targeted drug delivering. *Pharmacol. Res.* (2010) 62: 144-9.
- (19) Arruebo M, Fernández Pacheco R, Ibarra MR and Santamaría J. Magnetic nanoparticles for drug delivery. *Nano Today* (2007) 2: 22-32.
- (20) Revia RA and Zhang M. Magnetite nanoparticles for cancer diagnosis, treatment, and treatment monitoring: recent advances. *Mater. Today* (2016) 19: 157-68.
- (21) Arias J, Gallardo V, Gomez-Lopera S, Plaza R and Delgado A. Synthesis and characterization of poly (ethyl-2-cyanoacrylate) nanoparticles with a magnetic core. *J. Control. Release* (2001) 77: 309-21.
- (22) Boyer C, Whittaker MR, Bulmus V, Liu J and Davis TP. The design and utility of polymer stabilized iron-oxide nanoparticles for nanomedicine applications. *NPG Asia Materials* (2010) 2: 23-30.
- (23) Baalousha M, Manciuola A, Cumberland S, Kendall K and Lead JR. Aggregation and surface properties of iron oxide nanoparticles: influence of pH and natural organic matter. *Environ. Toxicol. Chem.* (2008) 27: 1875-82.
- (24) Turunen M, Olsson J and Dallner G. Metabolism and function of coenzyme Q. *Biochim. Biophys. Acta* (2004) 1660: 171-99.
- (25) Devun F, Walter L, Belliere J, Cottet Rousselle C, Leverve X and Fontaine E. Ubiquinone analogs: a mitochondrial permeability transition pore-dependent pathway to selective cell death. *PLoS One* (2010) 5: e11792.
- (26) Somers Edgar TJ and Rosengren RJ. Coenzyme Q0 induces apoptosis and modulates the cell cycle in estrogen receptor negative breast cancer cells. *Anticancer Drugs* (2009) 20: 33-40.
- (27) Yang HL, Lin MW, Korivi M, Wu JJ, Liao CH, Chang CT, Liao JW and Hseu YC. Coenzyme Q0 regulates NFκB/AP-1 activation and enhances Nrf₂ stabilization in attenuation of LPS-induced inflammation and redox imbalance: Evidence from *in-vitro* and *in-vivo* studies. *Biochim. Biophys. Acta* (2016) 1859: 246-61.
- (28) Yang HL, Korivi M, Lin MW, Chen SC, Chou CW and Hseu YC. Anti-angiogenic properties of coenzyme Q0 through downregulation of MMP-9/NF-κB and upregulation of HO-1 signaling in TNF-α-activated human endothelial cells. *Biochem. Pharmacol.* (2015) 98: 144-56.
- (29) Wang HM, Yang HL, Thiyagarajan V, Huang TH, Huang PJ, Chen SC, Liu JY, Hsu LS, Chang HW and Hseu YC. Coenzyme Q0 enhances ultraviolet B-induced apoptosis in human estrogen receptor-positive breast (MCF-7) cancer cells. *Integer Cancer Ther.* (2017) 16: 385-96.
- (30) Lakouraj MM, Hasantabar V, Tashakkorian H and Golpour M. Novel anticancer and antibacterial organometallic polymer based on ferrocene as a building block and xanthone bioactive scaffolds: Synthesis, characterization, and biological study. *Polymer Adv. Tech.* (2018) 29: 2784-96.
- (31) Khan F, Akhtar S, Almofty S, Almohazey D and Alomari M. FMSP-nanoparticles induced cell death on human breast adenocarcinoma cell line (MCF-7 Cells): Morphometric Analysis. *Biomolecules* (2018) 8: 32.
- (32) Kolosnjaj-Tabi J and Wilhelm C. Magnetic nanoparticles in cancer therapy: how can thermal approaches help? *Nanomedicine* (2017) 12: 573-5.
- (33) Allen TM. Ligand-targeted therapeutics in anticancer therapy. *Nat. Rev. Cancer* (2002) 2: 750-63.
- (34) Lenaz G, Fato R, Formiggini G and Genova ML. The role of Coenzyme Q in mitochondrial electron transport. *Mitochondrion* (2007) 7: S8-S33.
- (35) Chung CH, Yeh SC, Chen CJ and Lee KT. Coenzyme Q₀ from *antrodia cinnamomea* in submerged cultures induces reactive oxygen species-mediated apoptosis in a549 human lung cancer Cells. *Evid. Based Complement. Alternat. Med.* (2014) 2014: 246748.